

## Supporting Information

### Stacking-Faulted CDO Zeolite Nanosheets Efficient for Bulky Molecular Reactions

Qi Yang,<sup>a</sup> Yuhong Zhao,<sup>a</sup> Fangying Luo,<sup>a</sup> Shiqing Li,<sup>a</sup> Hao Xu,<sup>a</sup> Jingang Jiang,<sup>\*a</sup> Lu Han,<sup>\*b</sup> Peng Wu,<sup>\*a</sup>

<sup>a</sup> *Shanghai Key Lab of Green Chemistry and Chemical Processes, School of Chemistry and Molecular Engineering, East China Normal University, North Zhongshan Road 3663, Shanghai 200062, China. E-mail: pwu@chem.ecnu.edu.cn; jgjiang@chem.ecnu.edu.cn*

<sup>b</sup> *School of Chemical Science and Engineering, Tongji University, Siping Road 1239, Shanghai 200092, China. E-mail: luhan@tongji.edu.cn*

## Contents

Experimental section .....	1
1. Chemicals and reagents .....	1
2. Material Synthesis .....	1
2.1. Synthesis of OSDA .....	1
2.2. Synthesis of ECNU-57 .....	1
3. Characterization Methods .....	1
4. Catalytic reactions .....	2
5. Computation .....	3
6. Results and Discussion .....	4
Figure S1 .....	4
Figure S2 .....	5
Figure S3 .....	6
Figure S4 .....	7
Figure S5 .....	8
Figure S6 .....	9
Figure S7 .....	10
Figure S8 .....	11
Figure S9 .....	12
Figure S10 .....	13
Figure S11 .....	14
Figure S12 .....	15
Figure S13 .....	16
Figure S14 .....	17
Figure S15 .....	18
Table S1 .....	19
Table S2 .....	20
Table S3 .....	21
Table S4 .....	22
References .....	23

---

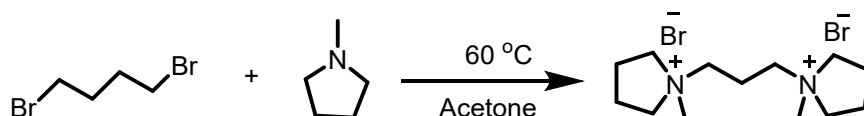
## Experimental section

### 1. Chemicals and reagents

All chemicals and reagents were obtained from commercial suppliers, such as 1,4-dibromobutane, 1-methylpyrrolidine, acetone, methanol, diethyl, tetraethyl orthosilicate (TEOS), hydrofluoric acid (HF), aluminum isopropoxide.

### 2. Material Synthesis

#### 2.1. Synthesis of OSDA



The organic structure-directing agent (OSDA) 1,4-*bis*(*N*-methylpyrrolidinium)-butane was synthesized by mixing 0.1 mol of 1,4-dibromobutane and 0.375 mol of 1-methylpyrrolidine in 100 mL of acetone and then stirred at 333 K for 12 h. The reaction mixture was then cooled to room temperature. The resultant solid product was washed several times with acetone, and its recrystallization was performed in methanol-diethyl ether mixture. After vacuum drying, a solid white product was obtained. The product was converted into hydroxide form by ion-exchanged with OH<sup>-</sup> resin. The final product 1,4-*bis*(*N*-methylpyrrolidinium) hydroxide concentration was determined by titration using potassium hydrogen phthalate with phenolphthalein as the indicator.

#### 2.2. Synthesis of ECNU-57

ECNU-57 was hydrothermally synthesized with 1,4-*bis*(*N*-methylpyrrolidinium) hydroxide as OSDA. In a typical synthesis, tetraethyl orthosilicate was hydrolyzed in aqueous solution of OSDA in a tared cup. Then, aluminum isopropoxide was added to the above mixture. The container was closed and stirred overnight to form a homogeneous sol-gel. The synthetic gel was then heated at 353 K to evaporate the ethanol and water until the molar ratio of H<sub>2</sub>O/SiO<sub>2</sub> reached 3.5. A desirable amount of HF was added and stirred until a thick gel was obtained. The final synthetic gel had a chemical composition of 1.0 SiO<sub>2</sub> : *x* Al<sub>2</sub>O<sub>3</sub> : 0.25 OSDA : *y* HF : *z* H<sub>2</sub>O, in which *x*, *y* and *z* were varied in the ranges of 0.008 – 0.1, 0 – 2 and 3.5 – 18.5, respectively. The gel was transferred to a 50 mL Teflon-lined stainless-steel autoclave and heated at 443 K for 7 days under static conditions. The product was collected by filtration, washing three times with water, and drying at 353 K for 12 h. The precursor was calcined in air at 823 K for 6 h to burn off the occluded organic species. When the synthetic gel had a molar composition of 1.0 SiO<sub>2</sub> : 0.016 Al<sub>2</sub>O<sub>3</sub> : 0.25 OSDA : 0.5 HF : 3.5 H<sub>2</sub>O, the product turned to be a nanosheet zeolite with 3D CDO topology, which was denoted as ECNU-57.

### 3. Characterization Methods

Powder X-ray diffraction (PXRD) was employed to check the structure and crystallinity of the zeolites, which were collected on a Rigaku Ultima IV diffractometer using Cu K<sub>α</sub> radiation at 35 kV and 25 mA in the 2θ angle range of 5 – 35° at a scanning speed of 1° min<sup>-1</sup>.

The elemental analyses for carbon and nitrogen contents were performed on an Elementar VarioEL III CHN elemental analyzer. The thermogravimetry (TG) and derivative thermogravimetry (DTG) analyses were carried out on a Mettler TGA/SDTA851e instrument at a ramping rate of 10 K min<sup>-1</sup> in air flow of 50 mL min<sup>-1</sup>.

Crystal morphology was determined using a Hitachi S-4800 scanning electron microscope (SEM) under an

accelerated voltage of 3 kV.

Transmission Electron Microscope (TEM) micrographs were obtained using a JEOL JEM-F200 FEG TEM operating at an accelerating voltage of 200 kV, together with a Gatan OneView IS camera that had a built-in drift correction function. An appropriate amount of solid powder was dispersed in ethanol to prepare low concentration suspension. Then, a drop of the above suspension was placed on a TEM grid to dry, then placed in the instrument chamber.

Textural properties of the samples were calculated from N<sub>2</sub> adsorption isotherms measured at 77 K on a BELSORP-MAX volumetric adsorption analyzer after the samples were activated at 573 K under vacuum for at least 3 h. The *t*-plot method was used to discriminate the microporosity and mesoporosity. The specific surface area was calculated with the Brunauer-Emmett-Teller method. The pore size distribution of samples was calculated by the BJH method.

Temperature-programmed desorption of ammonia (NH<sub>3</sub>-TPD) on a Micrometrics AutoChem II Chemisorption Analyzer was used to determine the acid amount. Typically, the sample (0.1 g) was pretreated in a helium stream (25 mL min<sup>-1</sup>) at 873 K for 1 h. The adsorption of NH<sub>3</sub> lasted for 1 h at 323 K. The sample was flushed with helium at 373 K for 2 h to remove physisorbed NH<sub>3</sub> from the catalyst surface. The TPD profiles were then recorded at a heating rate of 10 K min<sup>-1</sup> from 353 K to 1073 K. The Brønsted and Lewis acid sites of the sample were characterized by IR spectra of pyridine adsorption on a Nicolet Nexus 670 FT-IR spectrometer. After the evacuation of a self-supported sample wafer (50 mg in  $\phi$  2cm) at 723 K for 1 h, pyridine adsorption of the sample was carried out at 298 K for 0.5 h, and then IR spectra were collected after the evacuation at the required temperature.

<sup>29</sup>Si, <sup>13</sup>C and <sup>27</sup>Al MAS NMR spectra were performed on a VARIAN VNMRS 400WB NMR spectrometer. The <sup>13</sup>C CP MAS NMR spectra were determined at 75.5 MHz using adamantane as a chemical shift reference. The <sup>29</sup>Si CP MAS NMR spectra were measured on a VARIAN VNMRS400WB NMR spectrometer with a 7.5 mm T3HX probe at 79.43 MHz with a 60 s recycle delay at 3 kHz. The chemical shift was referred to as Q<sub>8</sub>M<sub>8</sub> ([[(CH<sub>3</sub>)<sub>3</sub>SiO]<sub>8</sub>SiO<sub>12</sub>]. The <sup>27</sup>Al MAS NMR spectra were recorded at 104.18 MHz, a spinning rate of 9 kHz, and a recycling delay of 4 s. KAl(SO<sub>4</sub>)<sub>2</sub>·12H<sub>2</sub>O was used as the reference for the chemical shift. The liquid-phase <sup>13</sup>C and <sup>1</sup>H NMR spectra of the organic structure-directing agent (OSDA) were recorded at 500 MHz on a Bruker Advance spectrometer. To investigate the interaction between organic and inorganic species in as-made ECNU-57, the solid-state HETCOR NMR experiments were carried out on a Bruker Advance III spectrometer (9.4 T), equipped with triple resonance 4-mm MAS probes under a magic-angle-spinning speed of 6 kHz. The NMR resonance frequencies for <sup>1</sup>H, <sup>13</sup>C, and <sup>29</sup>Si channels were 400.214, 100.613, and 79.495 MHz. The two-dimensional <sup>1</sup>H-<sup>13</sup>C and <sup>1</sup>H-<sup>29</sup>Si HETCOR NMR spectra were acquired with CP contact time of 2000  $\mu$ s and 5000  $\mu$ s, a recycle delay was set for 0.5 s and 0.75 s, respectively.

#### 4. Catalytic reactions

1,3,5-Triisopropyl benzene (TIPB) cracking reaction was carried out using a continuous flow system in a fixed-bed quartz reactor with an inner diameter of 15 mm. 0.2 g of catalyst was first activated at 773 K in a nitrogen flow (30 mL min<sup>-1</sup>) for 2 h under atmospheric pressure. Then TIPB was fed into the reactor with a rate of 1.7 mL h<sup>-1</sup> to start the cracking reaction at 623 K. The liquid products were collected regularly with an ice/water cold trap and analyzed on gas chromatography (Shimadzu 14B, FID detector, dB-Wax capillary column).

The Friedel-Crafts acylation reactions were carried out in the liquid phase with a round-bottom flask equipped with a condenser under stirring. An oil bath controlled the temperature. The exact reaction conditions were shown in the results and discussion. The reaction mixture was subjected to GC analysis (Shimadzu 14B, FID detector, dB-Wax capillary column) to determine the conversion and product selectivity.

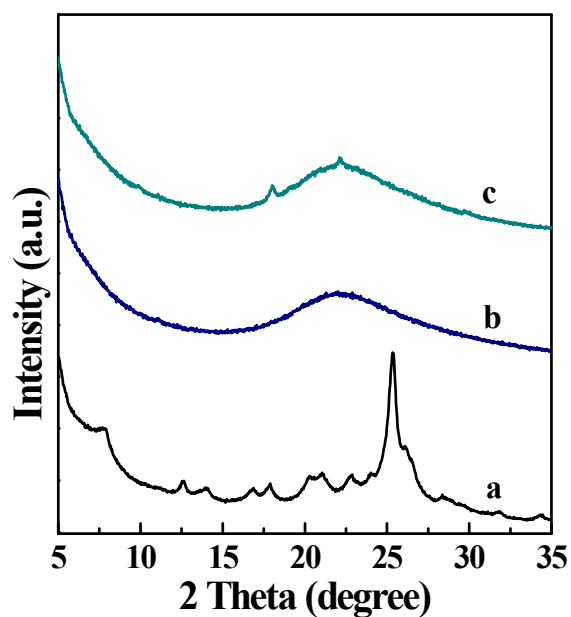
The alkylation of benzene with methanol, ethanol or isopropanol was carried out in a continuous flow fixed-bed reactor (8 mm) packed with 0.2 g of catalyst (particle sizes in the range 0.425-0.85 mm). Before the catalytic activity

testing, the catalyst was pretreated by N<sub>2</sub> flow at 723 K for 2 h and then the reactor was cooled down to the desired reaction temperatures (673 K). For the reactant feed, a mixture with a benzene alcohol ratio of 3 : 1 was introduced into the reactor using a pump (LANDE LD-P2020), and N<sub>2</sub> was used as carrier gas (30 mL min<sup>-1</sup>). The weight hourly space velocity of alcohol was 1.5 h<sup>-1</sup>. The reaction products were analyzed with a gas chromatograph (Tianmei GC-7900), an FID detector, and a DM-FFAP column (50 m × 0.53 mm). The conversion and the selectivity were calculated from gas chromatography results.

## 5. Computation

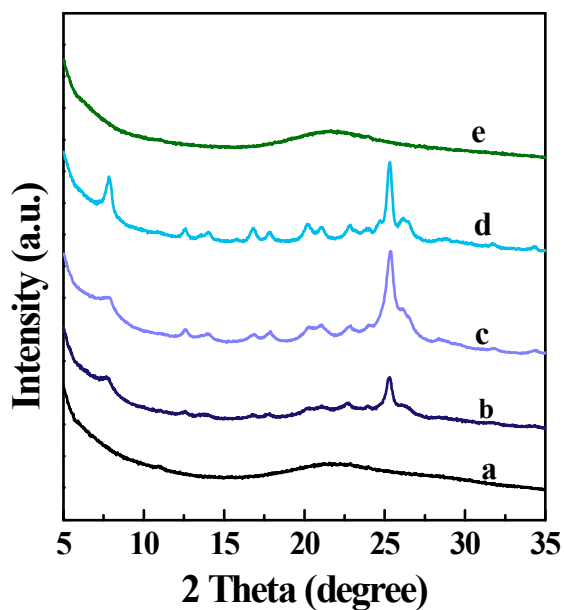
Molecular mechanics simulation, which was developed in the Forcite module of Materials Studio software, was used to analyze the position of the OSDAs in ECNU-57. The Dmol<sup>3</sup> module of Materials Studio determined the charge of OSDAs and energy. The CVFF forcefield utilized in the calculation assigned the charge to the layered framework. The charge of framework compensated the one of OSDAs. The framework structures of ECNU-57 were kept fixed throughout the calculations. In the calculations, periodic boundary conditions were used. Initially, the location of OSDAs in the layered CDO structure was manually docked. Simulated annealing was used to determine the most stable placement. The total energy minus the energy of the molecular sieve framework and the template energy equals the interaction energy. The Pawley refinement was calculated using the Reflex module of the Materials Studio.

## 6. Results and Discussion



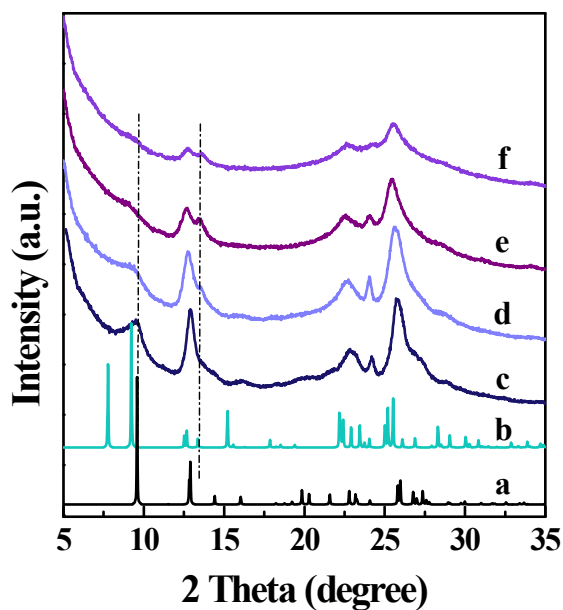
**Figure S1** PXRD patterns of the products obtained with  $H_2O/Si$  ratio of 3.5 (a), 8.5 (b), 18.5 (c). Other crystallization conditions:  $Si/Al = 30$ ,  $OSDA/Si = 0.25$ ,  $F/Si = 0.5$ , 443 K, 7 days, static.

*The PXRD pattern of samples synthesized with a  $H_2O/Si$  ratio of 3.5 showed the diffraction peaks characteristic of the CDO topology (Figure S1a). The only amorphous phase was obtained when the  $H_2O/Si$  ratio was more than 8.5 (Figure S1, b and c).*



**Figure S2** PXRD patterns of the products synthesized with F/Si ratio of 0 (a), 0.25 (b), 0.5 (c), 1 (d), 2 (e). Other crystallization conditions: Si/Al = 30, OSDA/Si = 0.25, H<sub>2</sub>O/Si = 3.5, 443 K, 7 days, static.

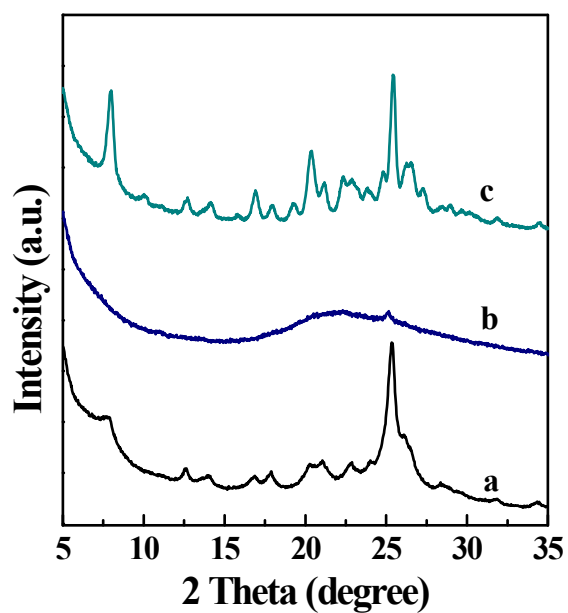
*The PXRD patterns of samples obtained with F/Si ratios of 0.25, 0.5 and 1 showed the diffraction peaks characteristic of the CDO topology (Figure S2, b-d). Amorphous phases were formed under F-free conditions or at a too high F/Si molar ratio of 2 (Figure S2 a and e).*



**Figure S3** PXRD patterns of simulated CDO (a), FER (b) and the calcined products obtained with Si/Al ratio of 30 (c), 20 (d), 10 (e), 5 (f). Other crystallization conditions: OSDA/Si = 0.25, H<sub>2</sub>O/Si = 3.5, F/Si = 0.5, 443 K, 7 days, static.

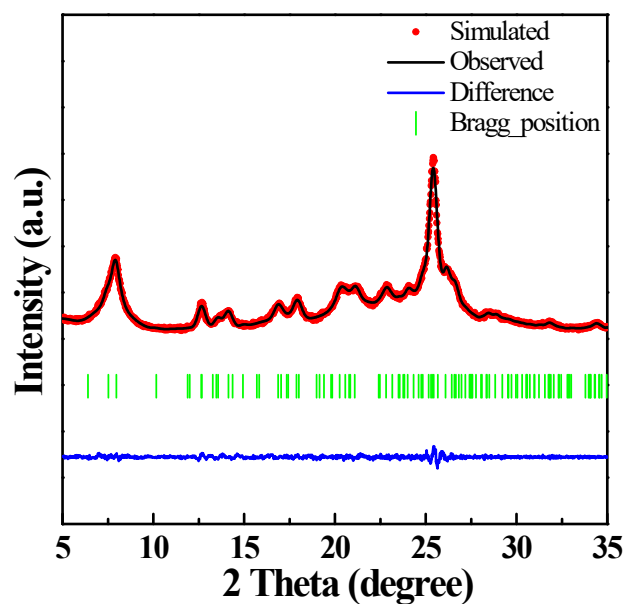
The PXRD pattern of the sample obtained with a Si/Al ratio of 30 showed the diffraction peaks characteristic of the CDO topology (Figure S3a and S3c). With the Si/Al ratios were reduced to 5-20, the characteristic peak in the low-angle region ( $2\theta = ca. 10^\circ$ ) gradually shifted to a lower area, and the new peak appeared in the region of  $2\theta = 13^\circ$  which was ascribed to FER topology, indicating that the products were composed of CDO and another phase FER (Figure S3b and d-f).





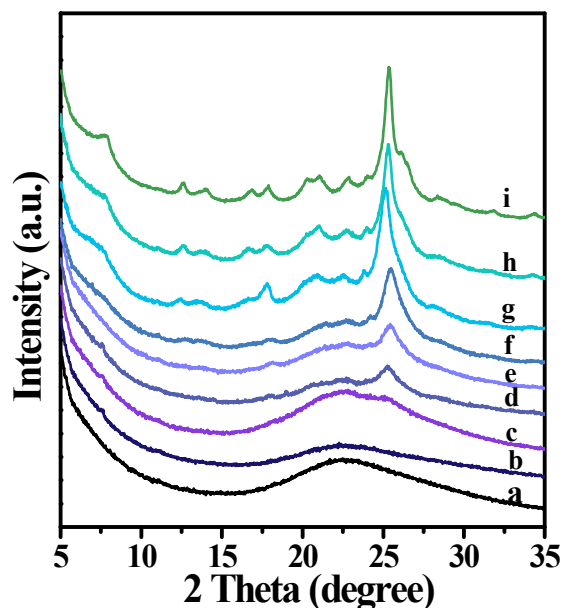
**Figure S4** PXR D patterns of the products obtained with various silicon sources of TEOS (a), fumed silica (b), colloidal silica (c). Other crystallization conditions: Si/Al = 30, OSDA/Si = 0.25, H<sub>2</sub>O/Si = 3.5, F/Si = 0.5, 443 K, 7 days, static.

*Only when TEOS was used as the silicon source, the product with the CDO topology was obtained (Figure S4a). The amorphous phase was formed when the silicon source was replaced with fumed silica (Figure S4b). And there would appear another phase with colloidal silica as silicon source (Figure S4c).*



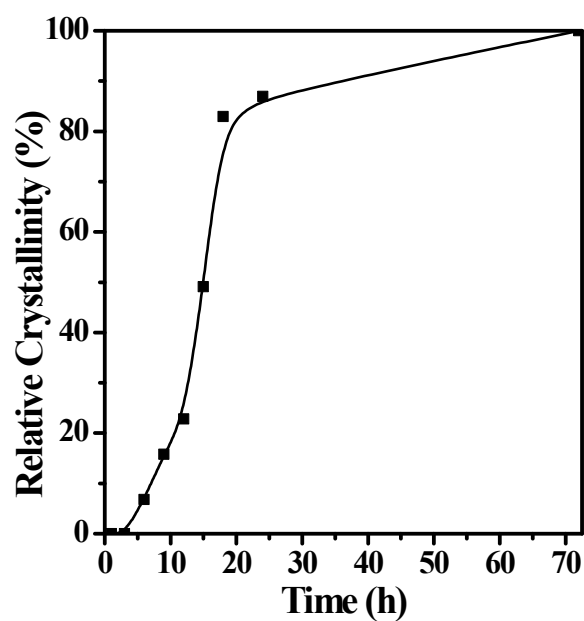
**Figure S5** Pawley refinement of the x-ray diffraction pattern of as-made ECNU-57 ( $\lambda = 1.5406 \text{ \AA}$ ). Data points (red) show the simulated patterns, solid line (black) along these points is the observed patterns, the different patterns at the bottom (blue), the vertical tick marks denote the positions of the Bragg reflections (green). (Rwp = 4.4%, Rwp(w/o bck) = 6.19%, Rp = 3.4%) ( $a = 7.4990(1) \text{ \AA}$ ,  $b = 22.5766(4) \text{ \AA}$ ,  $c = 14.1162(8) \text{ \AA}$ ;  $\alpha = \beta = \gamma = 90^\circ$ )

According to the cell parameters obtained from the Pawley refinement, it was concluded that as-made ECNU-57 was expanded along the *b*-axis and kept intact along the *a*-axis and *c*-axis, compared with typical CDO-type zeolite.



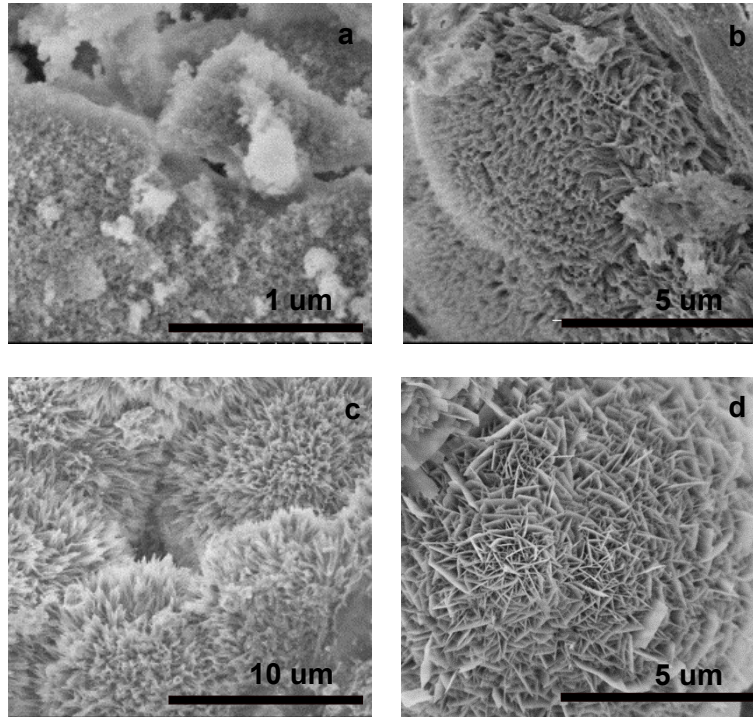
**Figure S6** PXRD patterns of the solids crystallized for a different period of time of 1 (a), 3 (b), 6 (c), 9 (d), 12 (e), 15 (f), 18 (g), 24 (h) and 72 (i) hours. The gel with the molar composition of 1.0 SiO<sub>2</sub> : 0.016 Al<sub>2</sub>O<sub>3</sub> : 0.25 OSDA : 0.5 HF : 3.5 H<sub>2</sub>O was synthesized at 170 °C with a static autoclave.

*The initial synthetic gel was amorphous aluminosilicate that did not show any X-ray diffraction peaks (Figure S6a). After 9 hours (Figure S6d), the characteristic peak appeared in the low-angle and high-angle regions of  $2\theta = 25^\circ$ - $30^\circ$ , probably due to the self-assembly of the hydrophobic tail segment in amphiphilic OSDA molecules. After heating for 18 hours, the crystalline CDO was formed together with coexisting amorphous phase (Figure S6g). Highly crystalline ECNU-57 with CDO structure was obtained after 72 hours (Figure S6i).*



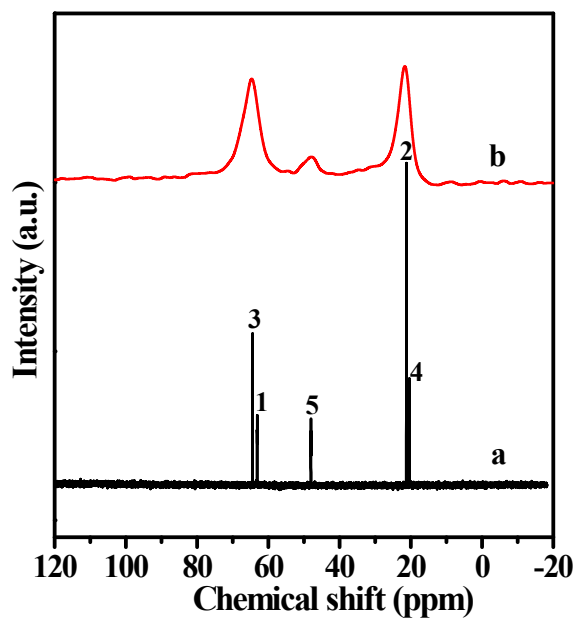
**Figure S7** Crystallization kinetic curve of the syntheses carried out with the molar composition of 1.0 SiO<sub>2</sub> : 0.016 Al<sub>2</sub>O<sub>3</sub> : 0.25 OSDA : 0.5 HF : 3.5 H<sub>2</sub>O at 170 °C in a static autoclave.

*As shown in Figure S7, a typical type S crystallization curve was observed with the induction period and the zeolite growth.*



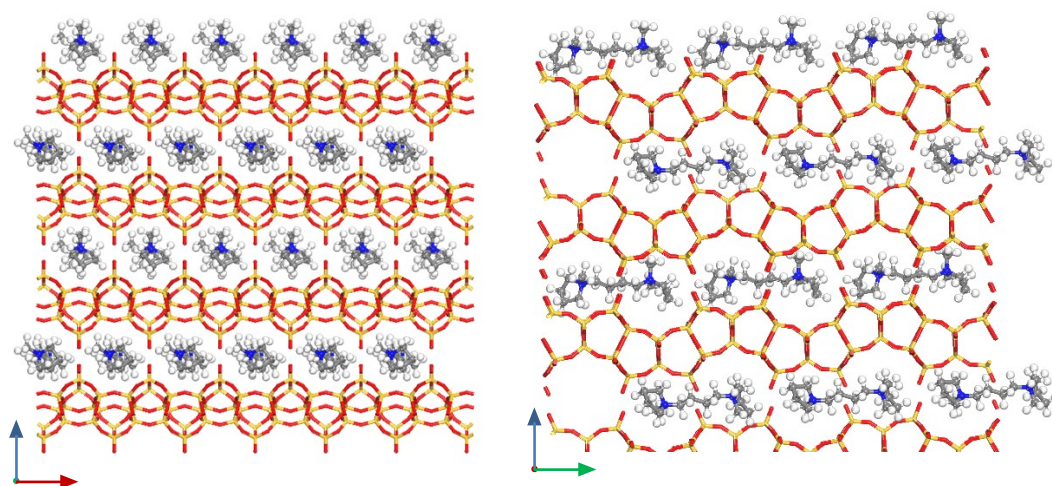
**Figure S8** SEM images of the as-made samples collected after the synthesis for a different crystallization time of 1 (a), 12 (b), 24 (c) and 72 (d) hours. Crystallization conditions: gel molar composition of 1.0 SiO<sub>2</sub> : 0.016 Al<sub>2</sub>O<sub>3</sub> : 0.25 OSDA : 0.5 HF : 3.5 H<sub>2</sub>O; synthesis performed at 170 °C with a static autoclave.

*As shown in Figure S8a, the amorphous aluminosilicate was observed at the beginning of the crystallization. The nanosheets morphology products emerged when the samples were crystallized for 12 h (Figure S8, b-d).*

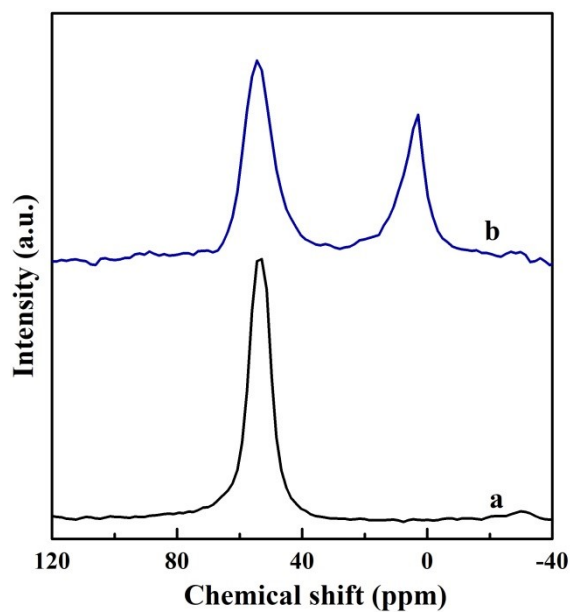


**Figure S9**  $^{13}\text{C}$  NMR spectra of OSDA 1,4-MPB showing the assignment of each resonance of 1,4-MPB in  $\text{D}_2\text{O}$  solution (a) and  $^1\text{H}$ - $^{13}\text{C}$  CP MAS NMR of as-made CDO-type ECNU-57 with 1,4-MPB occluded in the pores (b).

Figure S9 compared the  $^1\text{H}$ - $^{13}\text{C}$  CP MAS NMR spectrum of as-made ECNU-57 with the liquid  $^{13}\text{C}$  NMR spectrum of 1,4-MPB dibromide. Noticed that 1,4-MPB showed no difference in  $\text{D}_2\text{O}$  solution and H-C MAS. [1]The solid-state  $^{13}\text{C}$  CPMAS NMR spectrum of as-made ECNU-57 demonstrated that the OSDA remained intact after the crystallization.



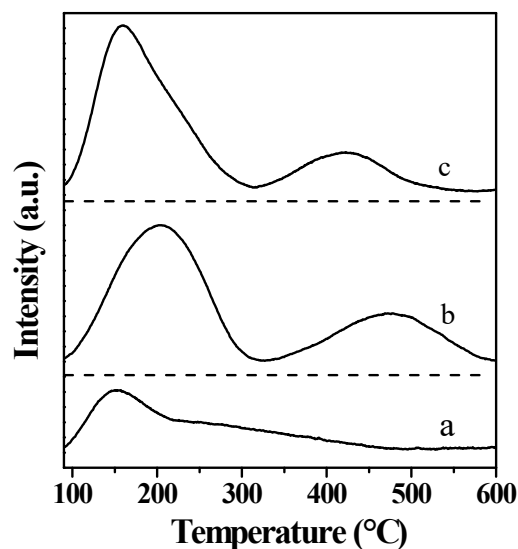
**Figure S10** Simulation geometry of stacking-ordered CDO occluded by OSDA cations in the intralayer structure.



**Figure S11**  $^{27}\text{Al}$  NMR spectra of as-made ECNU-57 (a) and calcined ECNU-57 (b).

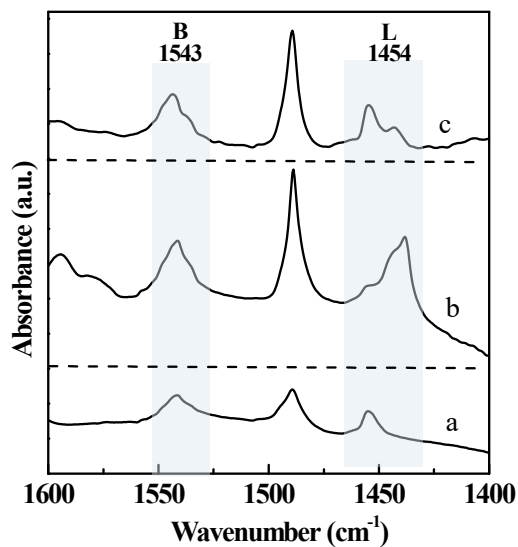
$^{27}\text{Al}$  MAS NMR spectra revealed the coordination environment of Al ions in as-made and calcined ECNU-57. The as-made material (Figure S11a) exhibited only one line around 53 ppm, typical of tetrahedral coordination Al. [2] A new peak at 0 ppm appeared upon calcination as a result of forming extra-framework octahedral Al species (Figure S11b). This implied that a part of the Al species was extruded from the CDO skeleton due to the thin nanosheets.





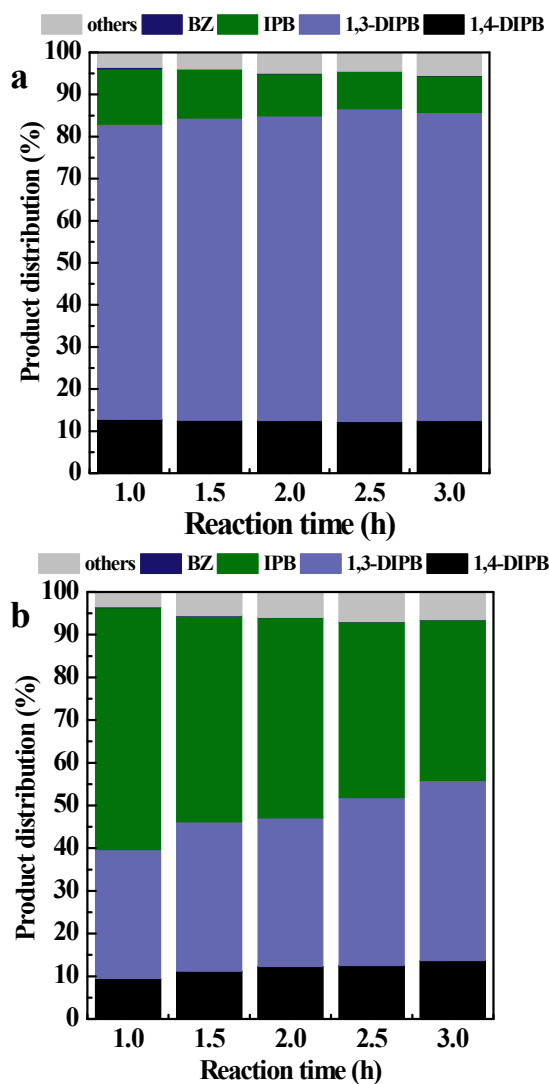
**Figure S12**  $\text{NH}_3$ -TPD profiles of ECNU-57 (a), FER (b) and \*BEA(c)

*Ammonia as a probe molecule interacts with the acid sites, and based on the desorption temperature and quantity during heating, weak, intermediate, and/or strong acid sites and their populations within the zeolite framework can be determined.<sup>[3]</sup> As shown in Figure S12, the  $\text{NH}_3$  desorption profiles of various materials showed the majority of desorption occurring below 600 °C. And the ECNU-57 possessed fewer acid sites than FER and \*BEA, and mainly had the acid sites with intermediate strength.*



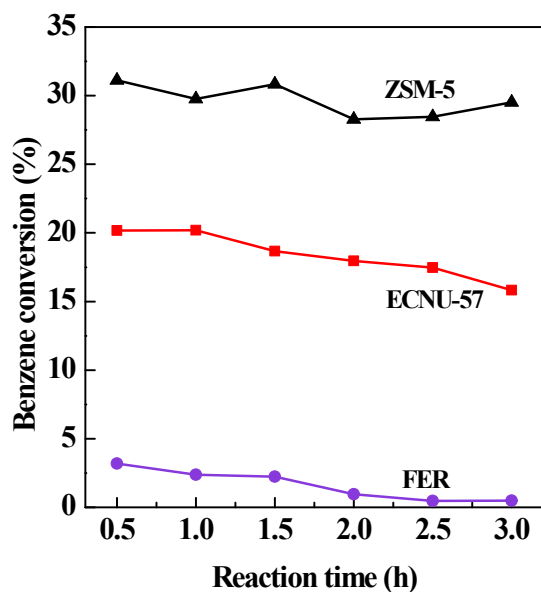
**Figure S13** IR spectra of pyridine adsorbed after evacuation performed at 150 °C on ECNU-57 (a), FER (b) and \*BEA (c)

Figure S13 illustrates the FTIR spectra of materials obtained after the pyridine adsorption at 25 °C, followed by desorption at 150 °C. The band around 1454  $\text{cm}^{-1}$  was assigned to pyridine adsorbed on the Lewis acid sites, and that around 1543  $\text{cm}^{-1}$  was due to pyridine adsorbed on the Brønsted acid sites. In general, the FER and \*BEA had more amounts of Brønsted acid sites and Lewis acid sites than ECNU-57.



**Figure S14** Product distribution of 1,3,5-TIPB cracking over FER (a) and \*BEA (b)

Figure S14 showed the product distribution results of various catalysts in the cracking reaction of 1,3,5-TIPB. The results showed that the product distribution of FER was similar to ECNU-57, which was dominated by 1,3-DIPB and 1,4-DIPB products, possibly because it had a similar layer structure. For \*BEA, the content of deep cracking product IPB was higher.



**Figure S15** Catalytic performances of benzene alkylation with ethanol over calcined ECNU-57, FER and ZSM-5. Reaction conditions: cat., 0.2 g; WHSV(ethanol), 1.4 h<sup>-1</sup>; N<sub>2</sub>, 30 mL min<sup>-1</sup>; temp., 673 K; benzene/alcohol ratio, 3.

*In the alkylation of benzene with ethanol, ECNU-57 showed a lower conversion of benzene than ZSM-5, but higher than FER. This might be due to its increased mesopore and external surface area, which was useful to promote the active site accessibility in comparison to FER. Nevertheless, the intracrystalline porosity and acidity of ECNU-57 were probably still inferior to MFI-type ZSM-5.*

**Table S1** Synthesis conditions for ECNU-57 and resulting phases.

Run	Gel composition (molar ratio)					Phase <sup>a</sup>
	SiO <sub>2</sub>	OSDA	Al <sub>2</sub> O <sub>3</sub>	HF	H <sub>2</sub> O	
1	1	0.25	0.008	0.50	3.5	ECNU-57
2	1	0.25	0.016	0.50	3.5	ECNU-57
3	1	0.25	0.025	0.50	3.5	FER+ECNU-57
4	1	0.25	0.050	0.50	3.5	FER+ECNU-57
5	1	0.25	0.100	0.50	3.5	FER
6	1	0.25	0.016	0.00	3.5	Amorphous
7	1	0.25	0.016	0.25	3.5	ECNU-57
8	1	0.25	0.016	1.00	3.5	ECNU-57
9	1	0.25	0.016	2.00	3.5	Amorphous
10	1	0.25	0.016	0.50	8.5	Amorphous
11	1	0.25	0.016	0.50	18.5	Amorphous
12 <sup>b</sup>	1	0.25	0.016	0.50	3.5	Amorphous
13 <sup>c</sup>	1	0.25	0.016	0.50	3.5	ECNU-57 + other

<sup>a</sup> All the products were synthesized at 170 °C for 7 days and calcined at 550 °C for 6 h. <sup>b</sup> Fumed silica as silicon source. <sup>c</sup> Colloidal silica as silicon source.

Table S1 listed the results from the syntheses obtained using OSDA with different Si/Al and H<sub>2</sub>O/Si molar ratios under the conditions described above. The phases provided were the only one obtained after repeated trials in each case. It could be seen that the gel composition ranged yielding ECNU-57 in the presence of OSDA, when the HF/Si ratio in the synthesis mixture was fixed to 0.5, for example, the Al/Si ratio successfully leading to the ECNU-57 formation with solid yields were found to be in the range 0.016-0.032. However, when increasing the Al/Si ratio in the gel to 0.050, we obtained another phase FER after calcined. Also, zeolite FER was always the phase crystallized from synthesis mixtures with Al/Si = 0.100. Table S1 also showed an increase in H<sub>2</sub>O content to 8.5 under the conditions where the synthesis of ECNU-57 proved an amorphous phase. Therefore, there appeared to be a reasonable amount of lattice charge introduced by Al substitution, together with a certain concentration level, in the crystallization of this CDO precursor. Furthermore, TEOS was the irreplaceable silicon source in this synthesis system. Table S1 also showed that replacing TEOS with an equivalent amount of fumed silica or colloidal silica as silicon source gave no crystalline phase or other phases even after heating at 170 °C for 7 days. This suggested that TEOS was irreplaceable in the synthesis mixture.

**Table S2** The physicochemical properties of materials.

Sample	Surface area (m <sup>2</sup> g <sup>-1</sup> )			Pore volume (cm <sup>3</sup> g <sup>-1</sup> )		
	S <sup>a</sup> <sub>total</sub>	S <sub>micro</sub>	S <sub>ext</sub>	V <sup>a</sup> <sub>total</sub>	V <sup>b</sup> <sub>micro</sub>	V <sub>meso</sub>
ECNU-57	486	229	257	0.75	0.07	0.68
*BEA	503	363	140	0.40	0.14	0.26
FER	285	240	45	0.26	0.11	0.15
ZSM-5	340	248	92	0.30	0.10	0.20

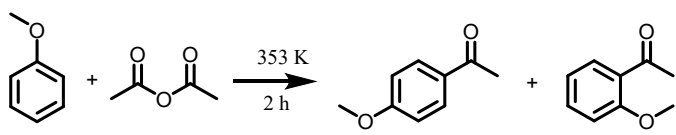
<sup>a</sup> Specific surface area was given by N<sub>2</sub> adsorption at 77 K and Brunauer-Emmett-Teller (BET) method.

<sup>b</sup> Given by *t*-plot.

**Table S3** Elemental analysis of the as-made ECNU-57 zeolite.

Sample	OSDA	C %	N %	C/N ratio
As-made ECNU-57	C/N=7	14.77	2.11	8.1

*The CHN elemental analysis gave a C/N molar ratio of 8.1 for as-made ECNU-57. It was consistent with or close to the theoretical value of the C/N ratio of 7 in OSDA, confirming that OSDA remained unchanged after high-temperature crystallization. The mass percentage of the CHN elements was 17.5 wt% by chemical elemental analysis, which was in agreement with the thermogravimetric analysis (16.7 wt%).*

**Table S4** Catalytic results for the acylation of anisole with acetic anhydride over different zeolites <sup>a</sup>

Catalyst	Topology	SSA <sup>b</sup> (m <sup>2</sup> g <sup>-1</sup> )	Si/Al	Conv.(%)
ECNU-57	CDO (8*8-MR)	486	22	87.1
H-FER	FER (8*10-MR)	285	15	24.4
ZSM-5	MFI (10*10-MR)	340	25	15.3
MCM-22	MWW (10*10-MR)	446	22	24.3

<sup>a</sup> Reaction conditions: cat., 0.1 g; anisole, 50 mmol; acetic anhydride, 5 mmol; temp., 353 K; time, 2 h. <sup>b</sup> Specific surface area given by nitrogen sorption at 77 K.

*As shown in Table S3, the conversion of acetic anhydride over ECNU-57 reached 87.1%, which was higher than other conventional zeolites. These results demonstrated that the enhanced exterior specific surface area of ECNU-57 had obvious advantages on the Friedel-Crafts acylation reactions.*



## References

- [1] S. B. Hong, G. Emily Lear, A. Paul, W. Zhou, P. A. Cox, C. Shin, J. Park, I. Nam, *J. Chem. Soc.*, **2004**, 126, 5817-5826.
- [2] G. Engelhardt, D. Michel, *High-Resolution Solid-State NMR of Silicates and Zeolites*, Wiley, Chichester, United Kingdom, **1987**.
- [3] J. Cha, T. Lee, Y. Lee, H. Jeong, Y. S. Jo, Y. Kim, S. W. Nam, J. Han, B. L. Ki, C. W. Yoon, H. Sohn, *Appl. Catal. B Environ.*, **2021**, 283, 119627.